

UPDATE ON THE ROLE OF COTTON STRUCTURE AND MORPHOLOGY IN DETERMINING FIBER STRENGTH

D.P. Thibodeaux and J.S. Moraitis
USDA-ARS-SRRC
New Orleans, LA

Abstract

Relationships between cotton fiber structure/morphology and strength have been examined for a wide range of physical and genetic properties. In particular, the relationships between the single fiber (MANTIS) strength and various bundle strength measurements including Stelometer and HVI were determined. In addition, relationships between the single fiber strength and the fiber physical/dimensional properties as obtained from the Advanced Fiber Information System (AFIS) and image analysis were determined. Tapered bundle strength as measured by the HVI correlated well with Stelometer flat bundle tenacity ($R^2 = 0.806$) but with a significant offset and non-unity slope. The average MANTIS breaking load could be predicted ($R^2 = 0.845$) by a linear combination of the average fiber wall area and perimeter as measured by AFIS. Both the Stelometer tenacity ($R^2 = 0.835$) and HVI breaking strength ($R^2 = 0.720$) are linearly proportional to the ratio of the MANTIS breaking load to the square of the projected ribbon width determined by the MANTIS electro-optical sensor. Both the Stelometer tenacity ($R^2 = 0.941$) and HVI breaking strength ($R^2 = 0.783$) can be expressed by a multi-linear relationship that includes the MANTIS breaking load and the projected fiber ribbon width.

Introduction

One of the major challenges for the cotton producer is to supply a raw material with consistent and uniform strength capable of competing with other natural and man-made textile fibers for use in the manufacturing of quality goods. This requires continued research on cotton to improve fiber strength. A significant recent advance in the technology of fiber strength measurements has been the development of the MANTIS single fiber tensile tester (Sasser et. al., 1991). In a more recent study (Hebert et. al., 1995), the latest version of MANTIS in which the hook over which the fiber is looped is replaced by a pair of clamps that grip the fiber ends was discussed. Also, significantly, an electro-optical system is included for measuring the projected ribbon width of each fiber prior to breaking. MANTIS single fiber strength and elongation was reported to correlate well with single fiber strength and elongation measured on the Instron tensile tester. Similarly, it was found that ribbon width was related to fiber fineness, that the MANTIS breaking strength decreased with increasing gauge length, and that the

convolution counts of cotton fibers can be predicted by the electro-optical measure of light scattering.

The purpose of the research reported herein was to develop improved understanding of MANTIS measurements of the breaking strength of single fibers and relate and interpret these results in terms of other physical property measurements (including AFIS and image analysis) and of bundle strength measurements. This should lead to an improved understanding of the relationships between fiber structure and performance, which will enable the cotton plant scientists to combine breeding, genetics, and cultural practices to produce cottons having superior strength.

Experimental

The general approach followed in this research was to: a) select cottons having a wide range of physical and genetic properties; b) conduct a series of experiments to determine the strength and physical/dimensional properties of these cottons; c) study the interrelationships among the single fiber and bundle strength measurements; and d) search for relations between the different measures of strength and the corresponding physical/dimensional properties.

The experimental procedures followed in this research are summarized below:

MANTIS

Single fiber tensile tester. The procedures outlined by (Hebert et. al., 1995) were followed which consisted of three repetitions of 150 single fiber breaks for each cotton. Parameters measured included the breaking load or force to break, T_b (g), and the ribbon width, RW (μm^2).

Stelometer

Flat bundle tester. Tests were performed according to standard procedures (ASTM D-1445-90). Values were obtained for an average of four bundle breaks. Factors measured included the breaking tenacity, $T1$ (g/Text) and the elongation to break, E (%).

High Volume Instrumentation

High volume instrument for rapid and automated measurements of fiber quality, used specifically in marketing and quality control of textile operations. Tests performed according to (ASTM D- 4605 - 86). Data was obtained on a Spinlab 900 HVI system and included bundle breaking strength (g/Text) and Micronaire. Results are based on four replications per sample.

AFIS

Advanced Fiber Information System. Specifically, the output from the "Fineness & Maturity" option was used for this work (Bradow et. al., 1996). The average of five replications of 5000 fibers each was calculated for each cotton. Measurements of interest here include average cell wall area (μm^2) and perimeter (μm) of the fiber samples.

Image Analysis

Sample were prepared by embedding in a polymer matrix and sectioning with an ultra microtome (Boylston, et. al., 1993). Image analysis was carried out on a Cambridge Instruments Model 970 Image Analysis system equipped with a Chalnicon scanner that was interfaced to a Nikon Optiphot2-POL light microscope operating with a 20x objective lens in the transmission mode (Thibodeaux, 1996). Measurements of the individual fiber cross-sections included average cell wall area (μm^2) and perimeter (μm) of the fiber samples. These data were based upon a minimum of 1000 sections per sample.

XRD

X-ray diffraction was used to measure the orientation of fibrillar crystallites about the fiber axis and the degree of crystallinity of cellulose in the cotton. Rigaku Instruments Model DMax B diffractometer equipped with a goniometer and special fiber bundle attachment was used. Procedures for measuring appropriate parameters on four replicates each of approximately 20 mg bundles of parallel fibers were followed using the method for measuring the orientation angle (Creeley et. al., 1956) and for the degree of crystallinity or crystallinity index (Segal et. al., 1959).

Materials

Samples included eight Egyptian cottons, seven American cottons (studied earlier at SRRC by N. El-Gawad and J. Hebert and five genetically related Texas supplied by John Gannaway. Results from the Texas cottons were first reported at the Beltwide Cotton Conferences (Faerber et. al., 1996). The 20 cottons were chosen for their genetic diversity and had a wide variation in their fiber properties (especially in the areas of length, strength, and fineness).

Results and Discussions

In describing the results of applying the various statistical methods to the 20 cottons, we have adapted a brief nomenclature for the variables under consideration. The variable nomenclatures along with their corresponding definitions are given in Table I. Since it is well known that there is a poor relationship between Tb and bundle strength measurements, our goal was to investigate the way in which Tb results could be combined with average fiber dimensional parameters determined by some of the established methods so as to correlate with both the Stelometer (T1) and the HVI. We considered linear combinations of Tb with other variables associated with each cotton. To accomplish this, a linear regression model was developed. Again, the specific procedure used was forward step-wise linear correlation. In the first instance, T1 is the dependent variable and Tb, RW, AIA, AAF, PIA, PAF, and MIC are the trial independent variables. Results of the correlation are given in Table II. Initially, the single variable with the highest R^2 is PIA, the image analysis perimeter, with $R^2=0.835$. The next most significant is RW

which adds $R^2=0.045$ to the model. The next step yields Tb with an additional partial $R^2=0.071$ with a cumulative R^2 of 0.952. The next step in the procedure shows that PIA may be dropped from model leaving the combination of Tb and RW accounting for a cumulative $R^2=0.952$. The excellence of this fit is depicted in Figure 1 which is a plot the actual values of T1 versus the corresponding values for T1 predicted from the equation

$$T1(\text{predicted})=62.28+2.66*Tb-3.95*RW \quad (1)$$

Next, HVI is the dependent variable and Tb, RW, AIA, AAF, PIA, PAF, and MIC are the trial independent variables. Results of the correlation are given in Table III. The single variable with the highest R^2 is RW with $R^2=0.471$. The next most significant is Tb which adds an additional R^2 of 0.312 to the model with a resulting cumulative R^2 of 0.783. These results are depicted in Figure 2 where we plot the actual values of HVI versus the corresponding values for HVI predicted from the equation

$$HVI(\text{predicted})=58.18+2.454*Tb-3.158*RW \quad (2)$$

The final consideration is that both the T1 and HVI parameters represent fiber tenacity or in effect, breaking stress where the force to break the bundle is normalized or divided by the corresponding bundle mass or linear density as discussed earlier. This compensates for differences in fiber cross-sectional area, perimeter, or linear density. Thus, another (and more logical) way of using Tb to predict bundle tenacity is to normalize the breaking load to account for different single fiber cross-sectional, dimensional qualities. In fact, we do not directly measure fiber cross sectional area, perimeter, or linear density, but average values are obtained from AFIS, Image Analysis, and Micronaire. Regression coefficients with several trial dimensional variables used as denominators for Tb are shown in Table IV. The trial variables consist of ratios of Tb to several dimensional variables including: AIA, AAF, PIA, PAF, PIA^2 , PAF^2 , RW, RW^2 , and MIC. TABLE V shows the values of R^2 and the corresponding levels of confidence (all data is significant at the 95% level or better). The highest correlation coefficient for the Stelometer T1 with a trial variable is obtained when using Tb/RW^2 which yields an R^2 of 0.907. Similarly, the highest correlation coefficient for the HVI bundle strength is also obtained when using Tb/RW^2 yielding an R^2 of 0.718. The relationship between T1 and $Tb/(RW^2)$ is illustrated in Figure 3. The trend line shown is given by the following equation

$$T1=2.66+666*Tb/(RW)^2 \quad (3)$$

The agreement between HVI and $Tb/(Tb/RW^2)$ for the cottons in this study is illustrated by the plot shown in Figure 4. There is some indication of increased scatter of

the points off of the trend line as compared with the data shown for T1 in Figure 5. Note that the y-intercept (12.32 gf/Tex) is even larger than was obtained with T1. The equation of this line is given by the following

$$HVI=12.455+530.49*Tb/(RW)^2 \quad (4)$$

Future Considerations

After reviewing the results it is clear that rather precise relationships exist between single fiber strength measurements (MANTIS) and conventional bundle measurements (Stelometer and HVI). In addition, measurements of fineness and maturity (by both AFIS and Image Analysis) are helpful in predicting fiber strength. One concern about the data is the significant offsets experienced in predicting Stelometer and HVI bundle strengths. Our research in the future shall center on three aspects:

- a) obtaining similar data on additional cottons;
- b) expanding our analysis to include considerations of MANTIS fiber crimp and the time aligned array analysis; and
- c) the inclusion of yarn performance data to check its predictability from these strength factors.

Summary and Conclusions

The following summarizes our findings from the studies of the 20 cottons:

1. Both the Stelometer tenacity (T1) and HVI breaking strength (HVI) can be expressed by a multi-linear relationship that includes the MANTIS breaking load (Tb) and the projected ribbon width (RW).
2. Both the Stelometer tenacity (T1) and HVI breaking strength (HVI) are linearly proportional to the ratio of the MANTIS breaking load (Tb) to the projected ribbon width (RW) squared determined by the MANTIS electro-optical sensor.

References Cited

ASTM Designation D 1445-90, Standard Test Method for Breaking Strength and Elongation of Cotton Fibers (Flat Bundle Method). Vol. 07.01.

ASTM Designation D 4605-86, Standard Test Methods for Measurement of Cotton Fibers by High Volume Instruments (HVI) (Spinlab System of Zellweger Uster, Inc.) Annual Book of ASTM Standards, Vol. 07.02.

Boylston, E.K., Thibodeaux, D.P., and Evans, J.P., Applying Microscopy to a Reference Method for Cotton Fiber Maturity, *Text. Res. J.*, **60**, 80-87 (1993).

Bradow, J.M., Hinojosa, O., Wartelle, L.H., Davidonis, G., Sassenrath-Cole, G.F., and Bauer, P.J., Applications of AFIS Fineness and Maturity Module and X-ray Fluorescence Spectroscopy in Fiber Maturity Evaluation, *Text. Res. J.*, **66**, 545-554 (1996).

Creely, J.J., Segal, L., and Ziifle, H.M., Determination of the Degree of Crystallite Orientation in Cotton Fibers by Means of the Recording X-ray Diffraction Spectrometer, *Text. Res. J.*, **26**, 786-795 (1956).

Faerber, C. and Gannaway, J., Fiber and Yarn Quality of New Texas Cottons, In: D.A. Richter and J. Armour (Editors), Proc. Beltwide Cotton Conf., San Antonio, TX, pp. 1383-1386 (1995).

Hebert, J.J., Thibodeaux, D.P., Shofner, F.M., Singletary, J.K., and Patelke, D.B., A New Single Fiber Tensile Tester, *Text. Res. J.*, **65**, 440-444 (1995).

Sasser, P. E., Shofner, F. M., Chu, Y. T., Shofner, C. K., and Townes, M. G., Interpretations of Single Fiber, Bundle, and Yarn Tenacity Data, *Text. Res. J.*, **61**, 681- 690 (1991).

Segal, L., Creely, J.J., Martin, A.E., and Conrad, C.M., An Empirical Method for Estimating the degree of Crystallinity of Native cellulose Using the Xray Diffractometer, *Text. Res. J.*, **29**, 786-794 (1959).

Thibodeaux, D.P. Status of Image Analysis Reference Method, Proceedings of the International Textile Manufacturers Federation (ITMF) Maturity Working Group, Bremen, Germany (1996).

Table 1. Definitions of variables used in this study.

Variable Nomenclature	Definition
T1	Stelometer Tenacity (gf/Tex)
HVI	HVI Strength (gf/Tex)
MIC	HVI Micronaire
Tb	Mantis Breaking Load (gf)
RW	Mantis Ribbon Width (um)
AAF	Cell Wall Area by AFIS (um ²)
PAF	Fiber Perimeter by AFIS (um)
AIA	Cell Wall Area by Image Analysis (um ²)
PIA	Fiber Perimeter by Image Analysis (um)
CRYST	Crystallinity Index (%)
XRAY	X-ray Orientation Angle (deg)

Table 2. Pearson correlation coefficients (r) and levels of significance for Mantis **Tb** with fiber properties.

PROPERTY	r	Prob > r
T1	0.373	0.105
HVI	0.380	0.098
RW	-0.0038	0.987
XRAY	-0.373	0.106
CRYST	-0.356	0.124
AAF	0.054	0.823
AIA	0.081	0.733
PAF	-0.354	0.126
PIA	-0.337	0.146
MIC	0.418	0.067

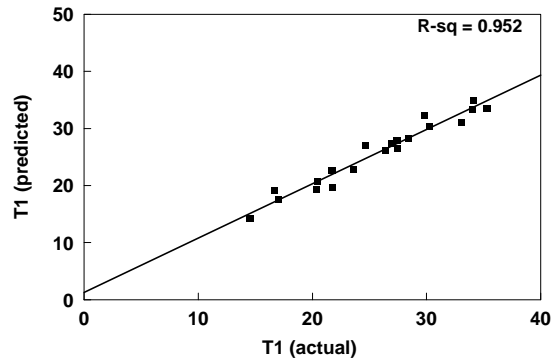


Figure 1. Stelometer tenacity predicted from linear combinations of **Tb** and **RW**.

Table 3. Results of forward step-wise linear correlation model for stelometer tenacity **T1** with **tb**, **rw**, **aia**, **aaf**, **pia**, **paf**, and **mic** as trial variables.

Trial Variable	Partial R ²	Model R ²	F	Prob>F
PIA	0.835	0.835	91.31	0.0001
Tb	0.045	0.881	7.101	0.0116
RW	0.071	0.952	36.293	0.0001
PIA (removed)	0.000	0.952	1.380	0.256

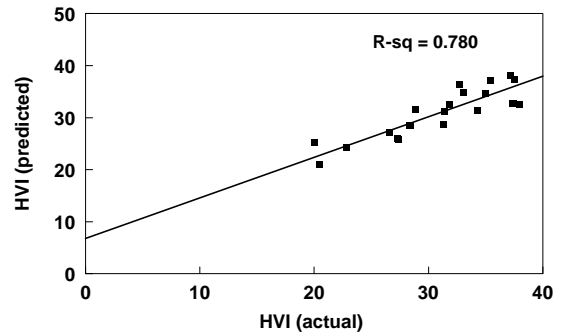


Figure 2. HVI strength predicted from linear combinations of **Tb** and **RW**.

Table 4. Results of forward step-wise linear correlation model for HVI strength with **tb**, **rw**, **aia**, **aaf**, **pia**, **paf**, and **mic** as trial variables.

Variable	Partial R ²	Model R ²	F	Prob>F
RW	0.6375	0.6375	31.66	0.0001
Tb	0.1422	0.7797	10.97	0.0041
PAF	0.0376	0.8174	3.29	0.0881 ^a
AAF	0.0355	0.8529	3.62	0.0766 ^a

^a Not significant at the 95% level of confidence.

Table 5. Pearson correlation coefficients (r) of several trial variables to find optimum relationship between mantis and bundle strength measurements.

TRIAL VARIABLE	T1	HVI
Tb/AIA	0.629	0.349
Tb/AAF	0.487	0.440
Tb/PIA	0.523	0.413
Tb/PAF	0.387	0.299
Tb/(PIA) ²	0.692	0.503
Tb/(PAF) ²	0.435	0.302
Tb/RW		0.690
Tb/(RW) ²	0.907	0.718
Tb/MIC	0.780	0.567

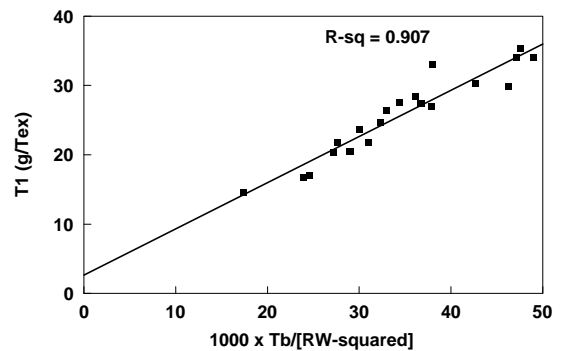


Figure 3. Stelometer tenacity predicted by Mantis **Tb**/[**RW**-squared].

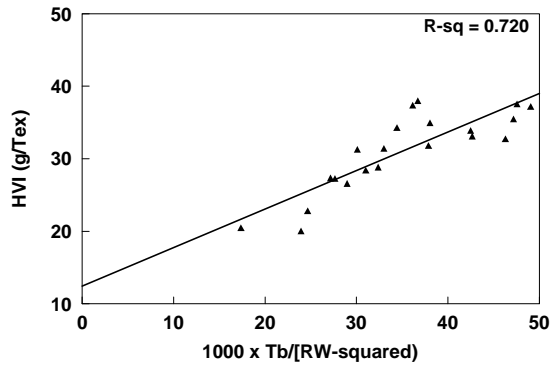


Figure 4. HVI strength predicted from Mantis Tb/[RW-squared].